ISSN 0003-701X, Applied Solar Energy, 2024, Vol. 60, No. 1, pp. 58–65. © Allerton Press, Inc., 2024.
Russian Text © The Author(s), 2024, published in Geliotekhnika, 2024, No. 1, pp. 74–82.

SOLAR ENERGY CONCENTRATORS

Optical Energy Characteristics of Large Solar Furnaces

Sh. I. Klychev[a], *, R. A. Zakhidov[b], S. A. Bakhramov[a], M. S. Paizullahanov[c], S. A. Orlov[a], L. S. Suvonova[d], Y. B. Sobirov[c], and S. Sh. Makhmudov[c]

[a] *Scientific and Technical Center with a Design Bureau and Pilot Production, Academy of Sciences of the Republic of Uzbekistan, Tashkent, 100125 Uzbekistan*

[b] *Tashkent State Technical University, Tashkent, Uzbekistan*

[c] *Institute of Materials Science, Academy of Sciences of the Republic of Uzbekistan, Tashkent, Uzbekistan*

[d] *National Research University, Tashkent, Uzbekistan*

**e-mail: klichevsh@list.ru*

Received July 14, 2023; revised September 28, 2023; accepted December 15, 2023

Abstract—The densities and fluxes of concentrated solar radiation in the focal plane of large solar furnaces (LSFs) are studied, taking into account the overall parameters, inaccuracies in the facets of the concentrator and heliostats, and shading and blocking the sun's rays by the fields of heliostats. It was found that LSFs can work effectively for 8 h a day throughout the year. It is shown that when the irradiance in the focus of the LSF is 0.6 from the limit, the root mean square error (RMS) of angular inaccuracies σ can be about 7 ang. min, and, if they are equal, each flat component (there are eight of them) can have deviations up to ± 4.2 ang. min, which if within σ, can be redistributed. The negative constant component of the inaccuracies of the curvature radius (integral inaccuracy) of the facet concentrator has a strong influence on the irradiance in the focus of the LSF, it should not be less than -0.2.

Keywords: Photometric radiation field theory, optical concentration of direct solar radiation, heliostats

DOI: 10.3103/S0003701X2460022X

INTRODUCTION

Solar furnaces, especially large solar furnaces (LSFs), with a power of up to hundreds of kW, are one of the important tools in materials science and are distinguished not only by high heating and cooling rates, but also by the ability to influence the properties of synthesized materials and the spectrum of solar radiation [1–7]. Currently, there are two LSFs operating in the world, one in Odeillo (France) and the other, in Parkent (Uzbekistan).

These LSFs are two-mirror faceted heliostat-paraboloid optical systems with a horizontal optical axis [8, 9].

In connection with the expansion of the range of problems solved at LSFs, more detailed knowledge of its optical-energy characteristics (OECs), in particular the flux (power) of solar radiation and its distribution in the focal plane, as well as their changes during the day and season of the year, is necessary.

The LSF OECs, in addition to the specular reflection factor (SRF), the facets of the concentrator and heliostats depend mainly on local and integral inaccuracies in the geometry of the facets and inaccuracies in their alignment. During the development of the design OECs of the LSF in Parkent (launched in 1987 [9]), the experience of constructing LSF in Odeillo was used.

The initial data for designing the LSF (concentration at the focus and the overall angular inaccuracy of the system) were developed by the group of Academician R.A. Zahidov [10–11]. In the process of developing the LSF, extensive work on research and analysis of the optical-geometric and energy parameters of the LSF was carried out at the Physico-Technical Institute, Academy of Sciences of the Republic of Uzbekistan under the leadership of Academician S.A. Azimov [9–11, 15–18].

After the launch of the LSF, the development of new methods for adjusting the facet concentrator and LSF heliostats were led by I.I. Pirmatov [19–21] and A.A. Abdurakhmanov [10]. A number of important results were obtained, and it was shown that: local facet inaccuracies are random, angular uncertainties contribute equally to the concentration reduction, and the total angular uncertainty can be represented as the sum of the RMS of the individual angular uncertainties.

At the same time, it follows that the analysis of LSF OECs, taking into account the facet and shape of the concentrator, the field parameters of the heliostats and the shading features falling on the heliostats (hereinafter shading) and reflected from the heliostats (hereinafter blocking) of sunlight, and the influence of individual inaccuracies of the facet and their no adjustments were carried out, with the exception of [12]. In

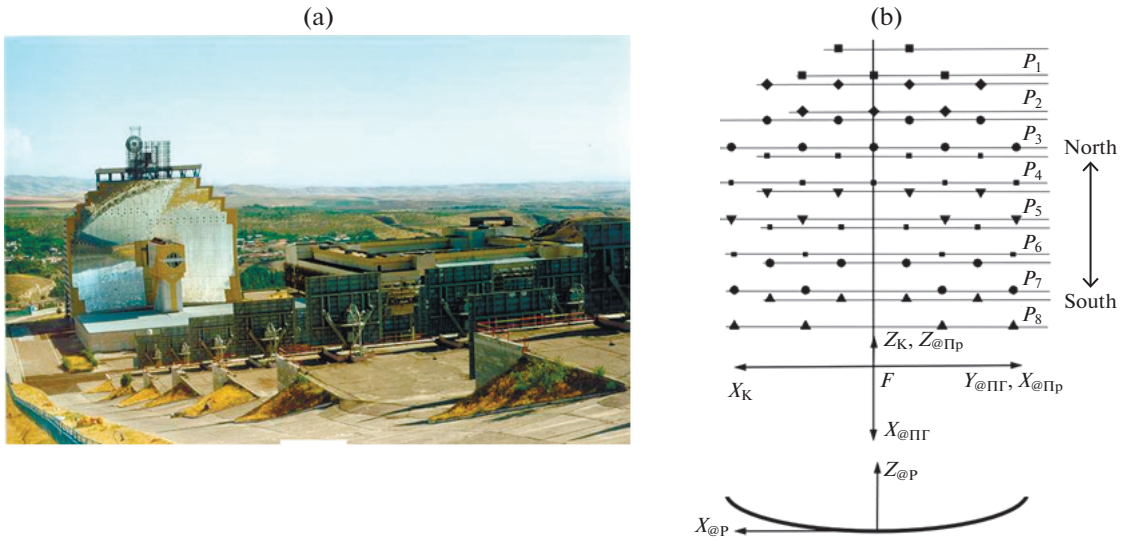

Fig. 1. General view of LSF [13] (a) and (b) location of heliostats (7.5 × 6.5 m^2, each) to scale (top view).

[12], irradiances at the focus of the LSF concentrator from individual heliostats were obtained, taking into account facet inaccuracies and blocking of solar rays in the heliostat field. The distribution of the concentrated solar flux in the focal plane of the system as a whole was not determined, the shading of solar rays by heliostats was not taken into account, and the influence on the OECs of the integral parameter of the inaccuracy of the facet concentrator as a whole was not considered, the deviation of the real radius of curvature of the facet from the calculated one.

Obtaining experimental data on OECs on existing LSFs is clearly insufficient, since they do not allow us to assess the state of LSFs relative to their limit values and, accordingly, the possibilities for their improvement. It can also be noted that the passport data for LSFs were assigned only on the basis of a generalized formula for the influence of inaccuracies on the irradiance at the focus [11], which did not take into account the facet of the concentrator and their integral inaccuracy, as well as changes in the effective area of the heliostat field during the day and year.

Objective—To study LSF OECs taking into account these factors and the influence of inaccuracies in the radius of curvature of the facet concentrator (integral geometry inaccuracy).

METHODS AND MATERIALS

We will conduct research on an analog close to the optical-geometric parameters of LSFs (Fig. 1). The laying of bevels on the paraboloid base of the concentrator was carried out as a projection of the central horizontal row of bevels onto the remaining sections of the paraboloid according to a latitudinal pattern with the centers of the bevels coinciding with the paraboloid base. It is also assumed that the facets of the concentrator are identical and square, and their geometry is spherical. In [13] it is indicated that the number of facets on the concentrator is about 10000, and on heliostats (62 heliostats), about 12000.

Within the framework of vector representations of the photometric theory of the radiation field [14], which were first used for the field of concentrated solar radiation in the works of R.A. Zakhidov and A.A. Weiner [10, 11], solar radiation density (irradiance) E_A at point A of the receiver of the facet concentrator during numerical integration is equal to [11]:

$$E_A = \sum_1^n \sum_1^N R_Z\, B(a)(n_M a)(n_A a)\frac{dS}{\rho^2}, \qquad (1)$$

where n is the number of facets on the hub, R_Z is the general coefficient of specular reflection of the system, N is the number of elementary normal areas dS on the facet with centers at point M, and unit normals n_M, n_A is the unit normal of the receiver at point A, ρ is the distance between points M and A and a is its unit vector, $B(a)$ is the brightness of the sun's ray along vector a. Usually, to reduce the calculation time (tens and hundreds of times, with the exception of diffusely reflecting surfaces), the return path of rays from the receiver points to the facets (concentrator) and then, after reflection, from the facets of the concentrator and heliostat to the solar disk is considered.

As is known, the variables in (1) must be specified in one of the coordinate systems (LSF CSs). Transitions between CSs and issues of unifying algorithms for calculating the characteristics of such systems, including in time, are described in sufficient detail by us in [15, 16]. The features of solution (1) for LSFs are formally manifested in additional blocks:

Table 1. Inaccuracies of the facet concentrator and LSF heliostats

No.	Type of inaccuracy	Designation	Characteristics
Concentrator			
1	Local inaccuracies in facet geometry, angle. min.	α_{KX}, α_{KY}	Maximum angular inaccuracies of normals: flat $\pm\alpha_{KXm}$, $\pm\alpha_{KYm}$, spatial $a_{TO} = \pm(a^2_{KXm} + a^2_{KXm})^{0.5}$ Standard deviation (RMS) σ:— uniform distribution—$\sigma_R = \alpha_{TO}/\sqrt{3}$, normal distribution—$\sigma_N = \alpha_{TO}/3$
2	Inaccuracies in the geometry of the facet as a whole (the facet is assumed to be spherical)	$dR = \Delta R/R_C$	$\Delta R = \pm(R_C - R_F)$ R_C, R_F—optimal and real radii of curvature of the facet, $R_C \approx 2\rho$ (ρ—the distance from the center of the facet to the focus), or the radius of the sphere adjacent to the paraboloid, $R_C = 1.0527P$ (P—focal parameter $P = 2f$, f—focal length [15, 16]
3	Inaccuracies in the adjustment of the facet of the concentrator, angle. min, or (′).	α_{jKX}, α_{jKY}	Maximum angular deviations of the optical axis of the facet from the exact position: flat—$\pm\alpha_{jKXm}$, $\pm\alpha_{jKYm}$, spatial—$\alpha_E = \pm(\alpha^2_{jKXm} + \alpha^2_{jKXm})^{0.5}$ σ: uniform—$\sigma_R = \alpha_{jK}/\sqrt{3}$, normal—$\sigma_N = \alpha_{jK}/3$
Heliostat			
4	Local inaccuracies of flat facets, angle. min.	α_{GX}, α_{GY}	Maximum angular inaccuracies of normals: flat—$\pm\alpha_{GXm}$, $\pm\alpha_{GYm}$, spatial—$a_G = \pm(a^2_{GXm} + a^2_{GXm})^{0.5}$ σ: uniform—$\sigma_R = \alpha_G/\sqrt{3}$, normal—$\sigma_G = \alpha_{TO}/3$
5	Inaccuracies in the adjustment of heliostat facets	α_{jGX}, α_{jGY}	Maximum angular deviations of bevels from the calculated position: flat—$\pm\alpha_{jGXm}$, $\pm\alpha_{jGYm}$, spatial—$a_{jG} = \pm(a^2_{jGXm} + a^2_{jGXm})^{0.5}$ σ: uniform—$\sigma_R = \alpha_{jG}/\sqrt{3}$, normal—$\sigma_G = \alpha_{jG}/3$

1. Block for determining the intersection of beam b (beam a reflected at point M) with a working heliostat.

2. A block that checks whether the beam is blocked by neighboring heliostats before it hits the working heliostat.

3. Block checking the shading of rays reflected from the working heliostat.

Heliostats are placed on eight shelves (P), see Fig. 1b. The distance between the rows of heliostats of two adjacent shelves is 5 m in height for (P_1–P_4) and 5.26 m in height for (P_4–P_8), and horizontally, 6.5 m. The distance between rows of heliostats on one shelf is 20 m, and between the centers of heliostats in one row is 12 m [13]. Inaccuracies in the geometry of the facet concentrator and LSF heliostats and their adjustment are characterized by the following parameters (Table 1) [15, 16].

Note that there are also inaccuracies in the tracking of heliostats to the Sun, but at the LSF in Parkent they do not exceed 0.5 ang. min. [17], and are not taken into account here. In the general case, there are also linear inaccuracies caused by the mismatch of the center of the rotation axes with the reflecting surface of the heliostat and angular errors between the azimuthal and zenithal axes and nonverticality of the azimuthal axis [18], which is important for software tracking, but for optical tracking they are automatically excluded (selected).

RESULTS AND DISCUSSION

In Figs. 2a and 2b, for an accurate concentrator and heliostats, taking into account the blocking and shadowing of rays in the heliostat field, the total irradiance from all shelves at the focus of the BSP E_S and fluxes Q at the receiver with dimensions 720 × 720 mm^2 are shown (number of points 289) and their changes during the day for different seasons of the year (δ). Figure 2b shows the contribution of E_S to separate shelves for δ = 23.5°. These curves are practically (±3%) symmetrical around noon, which was one of the ways to test the program. As can be seen, an accurate LSF can provide sufficiently high flux densities for at least 8 h in a day (±4 hours from noon) all year round. Note that the Uran type optical furnace pro-

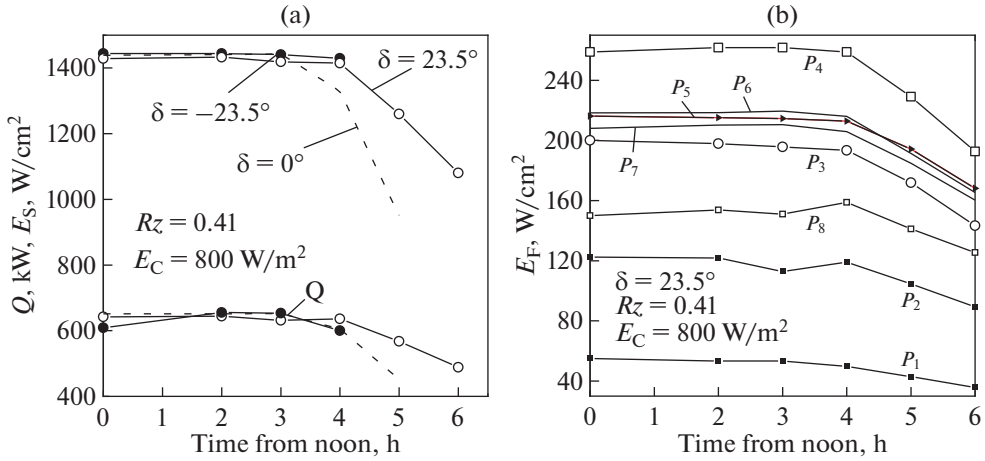

Fig. 2. Total irradiance E_S in focus and fluxes Q at a receiver with dimensions of 720 × 720 mm in the focal plane of an accurate LSF (a) and contribution to E_S of separate shelves (b).

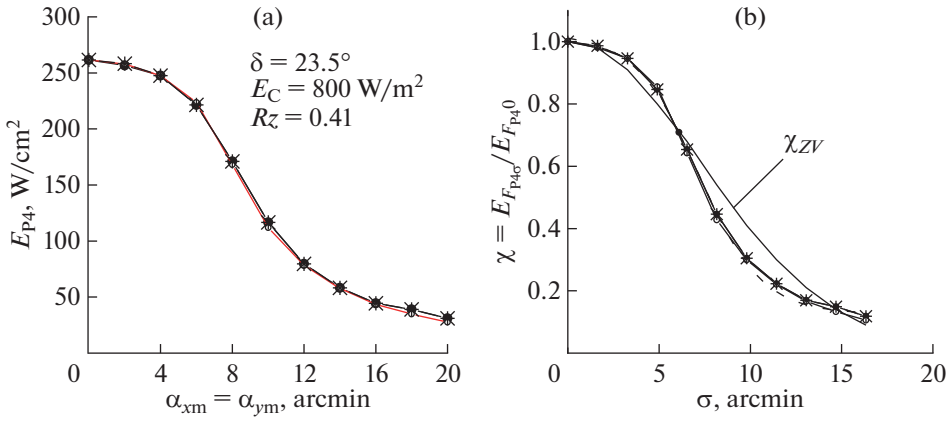

Fig. 3. The influence of random angular inaccuracies (1, 3–5, Table 1), distributed according to a uniform law on the focal irradiance from shelf 4, and the influence of inaccuracies individually—α_{xm}, α_{ym} (α_{TO}—●, αj_{TO}—○, α_G—*) and (b) their relative values χ from σ (χ_{ZV}— the pattern obtained in [10] for the normal distribution according to the beam scattering model

vides about 200 W/cm² at the focus [19], and with a secondary mirror, up to 500 W/cm² [20]. It is also clear that at the same E_s in winter, the irradiance can be the highest, which is due to the different nature of the orientation of the heliostats and the blocking and shadowing of rays. In practice, determining OECs in the presence of inaccuracies is important. It can be noted that blocking occurs mainly before ±2 h and does not disturb the effective area of the heliostats, and shading leads to a decrease in OECs and appears at the end of the day.

The influence of individual angular inaccuracies (1, 3–5 in Table 1) using the example of irradiance at the LSF focus from shelf 4 is shown in Fig. 3.

As can be seen, angular inaccuracies have the same effect on focal irradiances and are well approximated by the Origin program (sigmoidal distribution, dashed curve in Fig. 3b) and:

$$\chi = \frac{E_F}{E_{F0}} = A_2 + \frac{(A_1 - A_2)}{\left(1 + \exp\left(\frac{(\sigma - A_3)}{A_4}\right)\right)}, \quad (2)$$

where the coefficients are equal to $A_1 = 1.02586 \pm 0.01846$, $A_2 = 0.12569 \pm 0.01381$, $A_3 = 7.15381 \pm 0.14313$, $A_4 = 1.74335 \pm 0.13626$, E_F, E_{F0}— irradiation at the focus of the imprecise and precise concentrator, where E_F according to [10] is equal to:

$$E_F = \chi E_{F0} E_C R_Z. \quad (3)$$

Let us recall that the irradiance at the focus of an exact axisymmetric concentrator E_{F0} is equal to:

$$E_{F0} = E_C R_Z C_F \sin^2 U_0, \quad (4)$$

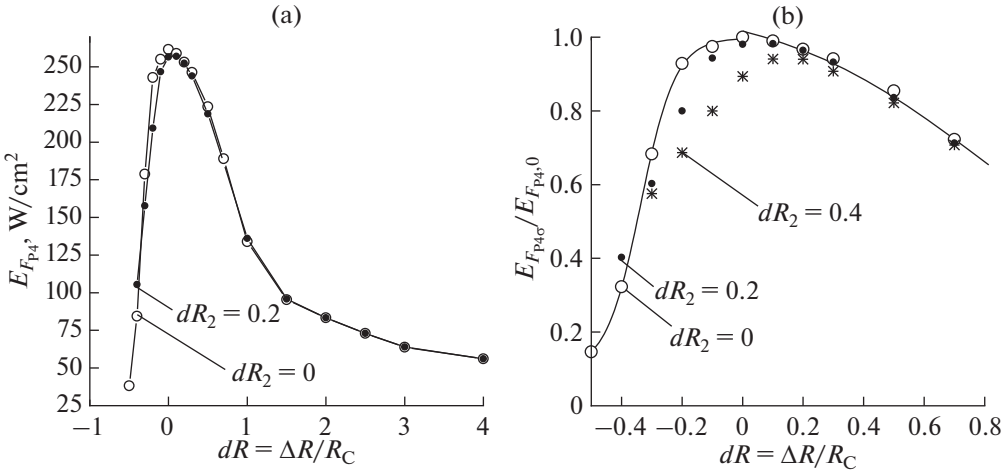

Fig. 4. The influence of constant dR inaccuracy on the focal irradiance of shelf 4 at different dR_2 (a) and its relative representation (solid curve, with $dR_2 = 0$) (b).

where U_0 is the concentrator opening angle, actual or effective [15, 21], C_F is the maximum concentration of solar rays at the focus of the paraboloid in air at $U_0 = 90°$, equal to:

$$C_F = \frac{1.2553\pi}{\left(\pi\varphi_0^2\right)} = 58\,041, \quad (5)$$

where 1.2553 is the ratio of the maximum density in the center of the solar disk to the average over the disk [15] with the brightness distribution over the solar disk according to Jose [22], $\pi\varphi_0{}^2$ is the projection of the solid angle of the solar disk, φ_0 is the angular radius of the solar disk (about 16 arcmin = 0.00465 rad).

Generalized uncertainty impact curve χ_{ZV} in Fig. 3b [10] has form:

$$\chi_{ZV} = \exp\left(-C_\sigma\sigma_i^2\right), \quad (6)$$

where $C\sigma = 9.2 \times 10^{-3}$ [1/ang min^2], σ_i is the RMS of individual or total angular inaccuracy, ang. min.

Difference between χ and χ_{ZV} are due to differences in models. Thus, when deriving (6), it was assumed that inaccuracies lead to blurring of the reflected solar cone, and the curves in Fig. 3 were obtained under the assumption that the reflected solar cone does not change, and inaccuracies lead only to a change in its direction. It can be seen that in the area acceptable for solar ovens σ ($\sigma < 8$ ang. min.), χ and χ_{ZV} are close enough.

Calculation estimates for other shelves showed that they have the same character as for shelf 4 (2). In this case, the maximum angular inaccuracies of the system α_S, taking into account the smallness of these angles, will be equal to a first approximation:

$$\alpha_S = \sqrt{\alpha_K^2 + \alpha_{JK}^2 + \alpha_\Gamma^2}. \quad (7)$$

Considering the connection between σ and α with their uniform distribution (see Table 1), we obtain:

$$\sigma_S = \sqrt{\sigma_K^2 + \sigma_{JK}^2 + \sigma_\Gamma^2}. \quad (8)$$

That is, in (2), σ can represent either a separate angular inaccuracy or a total one.

More difficult is assessing the influence of errors in the facet of the concentrator as a whole or the deviation of its radius of curvature ΔR or $e1$ relative value $dR = R_F/R_C$. In [12], it was assumed that dR is constant and only its sign changes randomly. Analysis shows that in this error it is advisable to distinguish between constant dR and random (dR_2) components, or determine the real radius of curvature of the facet in form:

$$R = R_\Phi(1 + dR + dR_2\left(2 \times \text{random} - 1\right), \quad (9)$$

where random is a standard generator of uniformly distributed random numbers from 0 to 1, or in (9), dR_2 varies from $-dR_2$ up to dR_2.

Limits of change of dR and dR_2 depend on bevel opening angle U_F (relative to the focus or center of curvature) [15, 20] and formally can vary from –1 to 1 [23, 24]. Figure 4a shows the effect of dR on irradiance at the focus from shelf 4 at different dR_2, and Fig. 4b shows its relative values, which no longer depend on E_S and R_Z.

This curve, the separate left and right parts, are also well approximated by an equation of form (2) with coefficients (Table 2):

As can be seen, even at small opening angles in LSFs, the facet of concentrator $U_F \approx 0.32°$ (from the center of curvature) the influence of dR is noticeably asymmetrical, and the positive tolerances on dR are significantly larger than the minus ones. Thus, with an acceptable decrease in E_F at 10%, negative dR should

Table 2. Coefficients of approximation error curves dR

Coefficient	Left part	Right part
A_1	0.09796 ± 0.01583	1.09364 ± 0.05201
A_2	0.99813 ± 0.00703	0.25651 ± 0.01526
A_3	−0.33635 ± 0.00337	0.77838 ± 0.05774
A_4	0.0573 ± 0.00292	0.3411 ± 0.0507

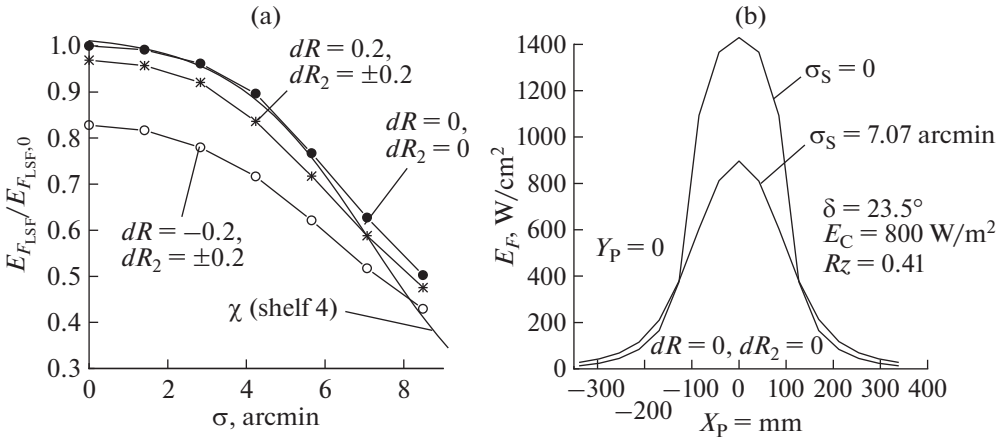

Fig. 5. Total irradiances at the LSF focus, taking into account blocking and shadowing, and the distribution of concentrated flux in the focal plane depending on the total σ and various dR and dR_2.

be less than −0.2, and positive, can be up to 0.5. It follows that when shaping bevels, it is very important to exclude the constant component of the inaccuracy of the radius of curvature of the bevels, especially their negative values, which can practically take place, given the small opening angles of the bevel concentrator on the LSF, while the random component can be within $dR_2 = \pm 0.2$.

Taking this into account, let us consider the influence of these inaccuracies on the total irradiance at the focus of the LSF concentrator as a whole from all field heliostats (Fig. 5a) and on the distribution of irradiance in the focal plane of the LSF (Fig. 5b).

It can be seen (Fig. 5a) that negative tolerances on dR actually have a more significant effect on E_F than positive ones. Yes, even with $\sigma = 0$ and $dR = -0.2$ and $dR_2 = \pm 0.2$, the irradiance at the focus drops by almost 20%, and at $dR = 0.2$ and $dR_2 = \pm 0.2$, by only 3%. Further with an increase in σ its influence begins to predominate, and the curves converge, however, even with $\sigma = 7'$, the influence of negative dR is 7%. It can also be seen that dependence χ for shelf 4 (Fig. 2b) up to $\sigma \le 7'$ also well describes the effect of angular inaccuracies on the total irradiance at the focus. At the same time, from Fig. 5b it is clear that inaccuracies primarily appear in the irradiance at the focus; this was also noted in [25]. When developing methods for shaping and adjusting bevel concentrators, first of all, it is necessary to use methods based on the control of focal irradiance, although, as noted above, due to their small opening angles of bevels, a noticeable change in irradiance in the vicinity of the focal zone occurs at sufficiently large dR.

The data allows us to assign values for individual angular inaccuracies. So, for example, from Fig. 5 it is clear that with $\sigma \approx 7$ ang. min., the irradiance at the focus can be about 0.6 of the maximum, and the total α_S will be $\alpha_S = \sigma\sqrt{3} = \pm 12.1$ ang. min. With identical individual angular inaccuracies (4 spatial in total, 8 flat), we have $\alpha_{xm} = \pm 4.3$ ang. min. This is a fairly large value, and within the limits of the overall inaccuracy, tolerances for individual inaccuracies can be redistributed taking into account the bevel manufacturing technology and the accuracy of their adjustment methods [13, 26–30].

CONCLUSIONS

1. Irradiances and fluxes in the focal plane of the LSF were determined, taking into account the main inaccuracies of the concentrator and heliostats, both from individual shelves with heliostats and totals, based on a developed calculation program that maximally takes into account the dimensions of the LSF optical system and its inaccuracies, as well as blocking and shading of solar rays in the heliostat field. It was

found that the LSF operating time can be up to 8 h per day at any time of the year.

2. It was found that the constant component of the radius of curvature of the facet *dR* (integral inaccuracy of the facet), especially its minus values, which should be less than –0.2, and positive ones can be up to 0.5, have a significant influence on the irradiance.

ACKNOWLEDGMENTS

The work was carried out within budget funding for research work of the Academy of Sciences of the Republic of Uzbekistan.

FUNDING

The work was carried out with budget financing of research work of the Academy of Sciences of the Republic of Uzbekistan.

CONFLICT OF INTEREST

The authors of this work declare that they have no conflicts of interest.

REFERENCES

1. Adylov, G.T., Kulagina, N.A., Mansurova, E.P., and Rumi, M.Kh., Glassy-crystalline materials on basis of cordierite glass produced in solar furnace, *Geliotekhnika,* 2004, no. 1, pp. 77–81.
2. Atabaev, I.G., Faiziev, Sh.A., Paizullakhanov, M., Shermatov Zh.Z., and Razhamatov, O., High-strength glass-ceramic materials synthesized in a large solar furnace, *Appl. Sol. Energy,* 2015, vol. 51, pp. 202–205.
3. Paizullakhanov, M.S., Suvonova, L.S., and Cherenda, N., Synthesis of a silicon carbide from natural raw material in a solar furnace, *High Temp. Mater. Process.: Int. Q. High-Technol. Plasma Process.,* 2023, vol. 27, p. i4. https://doi.org/10.1615/HighTempMatProc.2023048654
4. Paizullakhanov, M.S., Parpiev, O.R., Akbarov, R.Yu., and Suvanova, L.S., Features of the extraction of metals from waste in a solar furnace, *Appl. Sol. Energy,* 2022, vol. 58, no. 3, pp. 433–437.
5. Gulamova, D.D., Bobokulov, S.Kh., Turdiev, Zh.Sh., and Bakhronov, Kh.N., High-temperature superconductors of the $Bi_{1.7}Pb_{0.3}Sr_2Ca_{(n-1)}Cu_nO_y$ (n = 2–20) series synthesized under the influence of concentrated solar energy, *Appl. Sol. Energy,* 2018, vol. 54, pp. 358–360.
6. Akhmedov, M.K., Gulamova, D.D., Karimova, D.A., and Tadzhieva, D.F., Thermally resistant chamotte refractories based on the native Uzbekistan minerals, *Appl. Sol. Energy,* 2007, vol. 43, no. 2, pp. 109–112.
7. Klichev, Sh., Bakhramov, S., Abdurakhmanov, A., Fazilov, A., Payziyev, Sh., Ismanjanov, A., Bokoev, K., Dudko, J., and Klichev, Z., Two-stage concentrating systems for pumping of solar lasers, *Proc. SPIE,* 2008, vol. 6871.
8. Solar furnace with a capacity of 1000 kW of the French National Center for Scientific Research in Odeillo (design, parameters and first results of work), *Geliotekhnika,* 1974, no. 4, pp. 29–32.
9. Azimov, S.A., Scientific and production complex "Solntse". Bi-mirror polyheliostat solar oven with thermal power of 1000 kW, *Geliotekhnika,* 1987, no. 6, pp. 3–9.
10. Zakhidov, R.A., Umarov, G.Ya., and Vainer, A.A., Integral accuracy parameter of the heliostat-paraboloid system and its connection with mirror errors, *Geliotekhnika,* 1975, no. 3, pp. 31–34.
11. Zakhidov, R.A., Umarov, G.Ya., and Vainer, A.A., *Teoriya i raschet geliotekhnicheskikh kontsentriruyushchikh sistem* (Theory and Calculation of Solar Concentrating Systems), Tashkent: Fan, 1977.
12. Klychev, Sh.I., *Otchet po teme GNTP no. A-12-006* (Report on the Subject GNTP no. A-12-006).
13. Abdurakhmonov, A.A. and Abdurakhmonova, M.A., *Zerkal'no-kontsentriruyushchie sistemy dlya solnechnykh ustanovok i ikh effektivnost'* (Mirror-Concentrating Systems for Solar Installations and Their Efficiency), Tashkent: Universitet, 2022.
14. Gershun, A.A., *Izbrannye trudy po fotometrii i svetotekhnike* (Selected Works on Photometry and Lighting Engineering), Moscow: Gostekhizdat, 1958.
15. Klychev, Sh.I., *Doctoral (Eng.) Dissertation,* Tashkent, 2004.
16. Klychev, Sh.I., *Kontsentratory solnechnogo izlucheniya, modelirovanie i raschet* (Solar Radiation Concentrators, Modeling and Calculation), LAP Lambert Academic Publishing RU, 2016.
17. Atabaev, I.G., Akhatov, Zh.S., Mukhamediev, E.D., and Zievaddinov, Zh., Modernization of an automated controlling system for heliostat field of big solar furnace, *Appl. Sol. Energy,* 2016, vol. 52, no. 3, pp. 220–225.
18. Orlov, S.A. and Klychev, S.I., Compensation of axis errors of azimuth and zenith moving concentrators in programmable solar-tracking systems, *Appl. Sol. Energy,* 2018, vol. 54, pp. 61–64.
19. Eliseev, V.N. and Tovstonog, V.A., *Teploobmen i teplovye ispytaniya materialov i konstruktsii aerokosmicheskoi tekhniki pri radiatsionnom nagreve* (Heat Transfer and Thermal Testing of Materials and Structures of Aerospace Technology during Radiation Heating), Moscow: Mos. Gos. Tekh. Univ., 2014.
20. Ismanzhanov, A.I., Klychev, Sh.I., and Bokoev, K.A., *Vtorichnye kontsentratory solnechnykh teploenergeticheskikh ustanovok* (Secondary Concentrators of Solar Thermal Power Plants), Bishkek, 2015.
21. Klychev, Sh.I., Modeling of optical-energy characteristics of solar radiation concentrators, *Geliotekhnika,* 2002, no. 3, pp. 59–63.
22. Jose, P., The flux through the focal spot of a solar furnace, *Sol. Energy,* 1957, vol. 1, no. 4, pp. 12–22.
23. Umarov, G.Ya., et al., Technology for manufacturing inexpensive round-faceted concentrators from window glass, *Geliotekhnika,* 1969, no. 6, pp. 33–34.
24. Fedosov, I.V., *Geometricheskaya optika* (Geometric Optics), Saratov: Satellit, 2008.
25. Abdurakhmanov, A.A., Klychev Sh.Zh., Akhadov Zh.Z., and Mamatkosimov, M.A., Methodology for computational and experimental assessment of the characteris-

tics of mirror-concentrating systems, *Geliotekhnika,* 2005, no. 1, pp. 62–66.

26. Zakhidov, R.A., *Tekhnologiya i ispytaniya geliotekhnicheskikh kontsentriruyushchikh sistem* (Technology and Testing of Solar Concentrating Systems), Tashkent: Fan, 1978.
27. Zakhidov, R.A., Klychev, Sh.I., Bogdasarov, V.M., and Abdurakhmanov, A.A., Analysis of errors in heliostat adjustment methods, *Geliotekhnika,* 1983, no. 4, pp. 22–26.
28. Ikramov, A.M., Sobirov, Yu.B., and Abdurakhmanov, A.A., Adjustment and determination of the energy contribution of facet shaping of large-sized composite concentrators using a pinhole camera, *Geliotekhnika,* 2006, no. 3, pp. 57–62.
29. Kuchkarov, A.A., Sobirov, Yu.B., Kulakhmedov, N.N., Mamatkosimov, M.A., Akhadov, Zh.Z., and Abdurakhmanov, A.A., Adjustment of facets of flat and focusing heliostats, concentrators, and Fresnel mirror concentrating systems, *Appl. Sol. Energy,* 2015, vol. 51, pp. 151–155.
30. Sobirov, Yu., *Adjustment of flat bevels of heliostats of a large solar furnace*, *Eurasian Union Scientists,* 2021, pp. 36–41. https://doi.org/10.31618/ESU.2413-9335.2021.1.91.1471

SPELL: 1. OK